Chapter

What We Learned from Cavitation Bubbles in Microgravity

Mohamed Farhat

Abstract

The present chapter is about the *Flash and Splash* project, which is dedicated to the study of bubble dynamics in microgravity. The story of this project started in 2004 with a simple curiosity on how a cavitation bubble may behave within a water drop and evolved into an outstanding, internationally renowned science project as well as a wonderful human adventure. So far, we have participated in nine European Space Agency (ESA) parabolic flight campaigns (PFC) and made a significant progress in understanding the cavitation phenomenon. First, we investigated the dynamics of a cavitation bubble within a water drop and learned how the collapse may lead to the formation of a double jet. We discovered the formation of secondary cavitation due to the confinement of shockwaves within the drop. We used this result to propose a new path for erosion due to a high-speed impact of water drops on a solid surface. Then, we addressed the effect of gravity on bubble dynamics and came up with a unified framework to explain and predict key phenomena, such as microjets, shockwaves and luminescence. Parabolic flights gave us the unique opportunity to modulate the gravity-induced pressure gradient, which is crucial for the fate of a collapsing bubble.

Keywords: cavitation, bubble, shockwave, microjet, erosion

1. Introduction

I will always remember this sunny afternoon of September 2004 when I received in my office four talented students, D. Obreschkow, Ph. Kobel, N. Dorsaz and A. De Bosset, who had set themselves the goal of flying in microgravity. What else? The timing was perfect as, at that time, the European Space Agency (ESA) was organizing parabolic flight campaigns reserved for students. Still, to win their boarding pass, the students had to propose an innovative research project related to microgravity, and obviously, the competition was rather tough. I did not know how to help, as I had never been involved in such a crazy adventure. I politely explained that my research activity was about cavitation in hydraulic machines and there was nothing to do about it in a microgravity flight. However, this was not enough to discourage the students. A long and passionate brainstorming followed in search of the most credible project, or should I say the perfect excuse, to realize the dream of floating in microgravity. It was only by chance that, in the course of this rambling discussion, I mentioned an ongoing research project about the interesting dynamics

of a cavitation bubble within a liquid jet, performed in collaboration with the European Organization for Nuclear Research (CERN) [1]. Bingo! What if replaced the jet by a drop and proposed to study bubble dynamics within a water drop? Indeed, generating a centimeter spherical drop of water requires microgravity conditions. We could not find a better excuse! The students worked hard on their proposal, which ESA accepted straight away. Then, they worked even harder in building the experimental setup. The *Flash and Splash* project was born.

The beauty of the scientific research is that you never know where it may lead you. I did not know that this meeting of September 2004 was the start of a long and fruitful research activity on bubble dynamics in microgravity, which continues today. Following the first participation in the students flight campaign, we took part in eight research campaigns with the involvement of four PhD students, M. Tinguely [2], O. Supponen [3], A. Sieber and D. Preso with many other master students and technicians. This innovative and exciting research, which received financial supports from the Swiss National Science Foundation, the European Union and many other governmental and private institutions, produced a strong impact within the scientific community and beyond. It received many awards and recognitions as well. *Flash and Splash* is not only a successful research project, it is also a great human adventure made of friendship, generosity and unforgettable memories.

In the following sections, I will give an overview on the cavitation phenomenon, which motivates the actual research. I will then summarize the technical aspects and main results related to bubble dynamics in microgravity.

2. What is cavitation?

Cavitation is the formation and collapse of vapor bubbles within a liquid due to a transient pressure drop. It may occur in a variety of hydraulic systems such as water turbines and pumps, ship propellers and space rocket inducers. In these applications, cavitation is a “nightmare” for design engineers and operators because it may lead to severe erosion, noise and vibration as well as alteration of hydrodynamic performances.

In the particular case of hydropower generation, the occurrence of cavitation in water turbines often requires periodic shutdowns of the power plant to allow for inspections and repairs, which increase significantly the operational cost. **Figure 1** illustrates the different types of cavitation in hydraulic machines as well as a pump impeller severely eroded by cavitation.

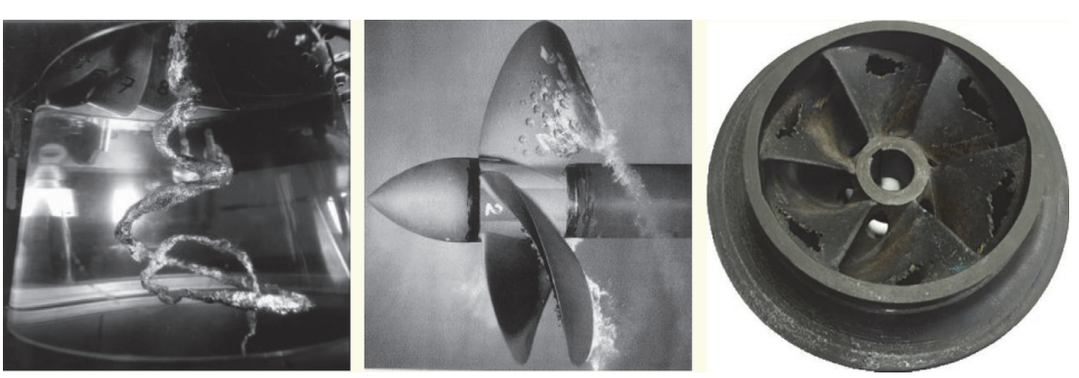

Figure 1.
Left: cavitating vortex in a Francis turbine, operating at off-design conditions; middle: cavitation in a ship propeller (courtesy Franc et al. [4]); right: pump impeller heavily eroded by cavitation.

In the course of the past 100 years, the booming development of hydropower and pumped storage power plants around the world and the need for faster and quieter ships and submarines have fuelled an intense and sustained research activity on the cavitation issue. This led to a better understanding of the physics behind the transient growth and collapse of vapor cavities in flowing liquids and the mechanism of induced erosion and noise. It is well known nowadays that cavitation erosion is due to vapor bubbles, which nucleate and grow in low-pressure area and then collapse violently as they move to a higher-pressure zone. Therefore, the cavitation aggressiveness is influenced by the minimum pressure, which governs the size of the vapor cavity, as well as the downstream pressure gradient and the liquid velocity, which together characterize the violence of the collapse. Despite the progress made so far, many issues related to cavitation remain unanswered.

High-speed sailing is another field where cavitation is a challenging issue and a limiting factor. In fact, any submerged body will face cavitation when it travels faster than a threshold speed. Interestingly, this also holds for fishes, whose speed is likely limited by cavitation. The fact that only few predatory fishes, e.g. sailfish and black marlin, can swim faster than 40 knots is due to cavitation occurrence. We have illustrated on **Figure 2** the case of the *Hydroptère* boat, which sat the speed sailing record to 50.17 knots in September 2009 in Hyères (France). Beyond a threshold speed, this "flying boat" uses lifting foils to raise its hull out of the free surface, leading to a significant drag reduction. We have presented on the same figure the experimental evidence of cavitation occurrence on the lifting foil at reduced scale, which we have performed in the high-speed cavitation tunnel of the *Ecole Polytechnique Fédérale de Lausanne* (EPFL). Our investigations reveal that the cavitation occurrence is responsible for a sharp drop of the lift force, which increases the risk of the boat capsizing. We have also learned that it is almost impossible to avoid cavitation when the speed is beyond ~40 knots. Therefore, any attempt to break the actual speed sailing record (55.32 knots established by Vestas Sailrocket team in 2012) requires accommodation of cavitation. This is exactly what an EPFL student's team, among others, is trying to achieve in the frame of an ongoing project (SP80) with the help of supercavitating foils.

An interesting example of cavitation in nature is that of snapping shrimps, which are among the noisiest underwater creatures. Colonies of such crustaceans can produce an intense and wideband noise that interferes with sonars and underwater communication. Snapping shrimps, also called pistol shrimps, use the extraordinary power of cavitation to defend their territory and hunt prey animals. Upon an extremely rapid closure of their large claw, a transient high-speed jet develops and forms vortex rings. The resulting pressure drop within these vortices leads to the growth and collapse of toroidal vapor cavities [5].

From a fundamental viewpoint, the first mathematical model was proposed by Lord Rayleigh in 1917 [6], who used the potential flow theory to provide a

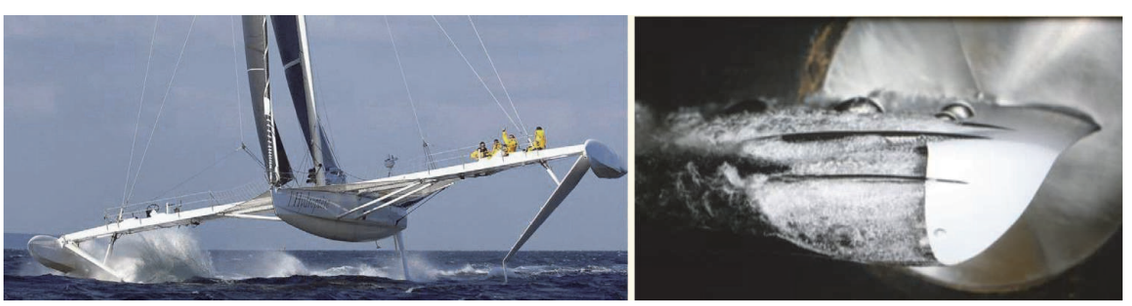

Figure 2.
Left: the Hydroptère sailing boat (courtesy A. Thébaut) and right: evidence of cavitation on a model of the Hydroptère *lifting foil.*

remarkable prediction of the collapse time of an empty spherical cavity in an incompressible fluid. He also predicted that before the cavity closes, the pressure rises very high in the fluid close to the interface. Since then, more sophisticated models have been proposed, taking into account the phase transition, viscosity, surface tension, gas content and compressibility. Besides, a large number of experimental investigations took profit from the development of pulsed lasers to generate spherical bubbles on-demand and unveiled peculiar phenomena. **Figure 3** illustrates a typical growth and collapse of a cavitation bubble induced by a pulsed laser in still water along with the evolution of the bubble radius and the signal of pressure alteration, measured far from the bubble centre. We can observe how the hot plasma induced by the laser leads to an explosive growth of a bubble, filled with gas and water vapor. As the bubble expands, it cools down and reaches a maximum radius of ~4 mm before it collapses violently. The bubble lifetime is less than a millisecond. During the collapse phase, the water vapor condenses while the noncondensable gas is strongly pressurized and heated up before it rebounds and collapses again with a decreasing intensity. Interestingly, the Rayleigh theory predicts an infinite velocity and hence infinite energy densities at the end of the collapse. According to general relativity, such a singularity would generate a black hole—a scary scenario that, fortunately, never happens because a plethora of nonlinear effects, such as liquid compressibility, heating and radiative energy transfer, halt the catastrophic collapse well before relativistic physics becomes noticeable.

Figure 3 illustrates also the emission of intense shockwaves at the initial and final stages of bubble growth and collapse. What makes these shockwaves visible is the sharp density gradient at their front, which alters the refraction index and deviates light. Shockwaves are attributed to the supersonic motion of the bubble interface and the liquid compressibility and may reach Giga Pascal amplitudes.

Another fascinating aspect of collapsing bubbles is their capacity to generate light (luminescence), as illustrated on **Figure 3**. This phenomenon was first observed in the context of bubbles excited by ultrasound in 1933. It is due to a spectacular compression of the noncondensable gas, which heats up to such a degree that light is emitted in the form of a nanosecond flash. Many experimental and theoretical studies have been devoted to luminescence to better understand its mechanism. It is well accepted that the temperature of the gas enclosed in a spherically collapsing bubble may reach 10,000°K, which leads to the generation of free radicals that recombine and radiate light. This result raised a hope that nuclear

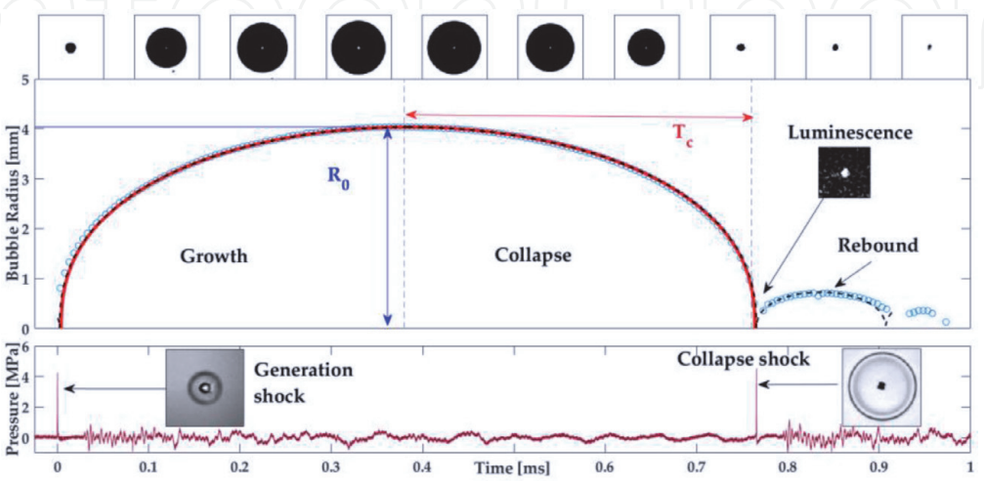

Figure 3.
Top: visualization of a laser-induced bubble dynamics (112 μs inter-frame); middle: measured bubble radius (blue circles), along with theoretical predictions; bottom: pressure signal measured far from the bubble centre (reproduced from [3]).

fusion might occur inside a collapsing bubble, provided that the bubble is large enough and remains spherical. It is hard to meet these requirements on earth, because large bubbles deform significantly in the presence of the gravity-induced pressure gradient. After many attempts to increase the temperature reached in the centre of a collapsing bubble, the objective of nuclear fusion was abandoned amid a large controversy. Yet, research on luminescence continues, motivated by its ability to act as a catalytic host for chemical reactions with promising outcomes for sterilization, nanomaterials, cancer therapy and more.

Moreover, it is also well known that when a bubble is set to grow and collapse near a rigid wall, hydrodynamic instabilities develop at the bubble interface, due to pressure anisotropy. This leads to the generation of a high-speed microjet directed towards the boundary. When the solid surface is replaced by a free surface, the microjet develops in opposite direction, and the bubble moves away from the surface while a counter-jet emerges from the free surface (see **Figure 4**). The cavitation erosion is believed to originate from a combined action of the shockwaves and microjets. The current research is still struggling to further understand and predict erosion due to collapsing bubbles.

What makes cavitation bubbles fascinating is their extraordinary ability to focus energy and produce the powerful phenomena reported earlier. Cavitation remains a hot topic of research because of its multidisciplinary aspect, which involves multiscale fluid and solid mechanics, plasma physics, thermodynamics and chemistry, with a strong interaction between them. While cavitation bubbles were historically associated with negative outcomes, e.g. noise, vibration and erosion in hydraulic systems, more and more efforts are dedicated to take profit from their power in a variety of applications. This includes surface cleaning, material and food processing and water treatment. There is also a growing interest in using cavitation bubbles in medicine, e.g. treatment of musculoskeletal system disease, breakage of kidney stones, drug delivery, cancer cell treatment, etc. All these promising developments require a better knowledge of cavitation bubbles to allow for mastering their effects.

3. Microgravity experiments: what for?

We have initiated 15 years ago a research programme to address the knowledge gaps associated with cavitation bubble dynamics with the help of a state-of-the-art instrumentation. The focus was accorded to the distribution of the bubble's energy into its various collapse phenomena, namely, the microjets, shockwaves, rebound and luminescence. To this end, we built a versatile experimental setup, which produces initially spherical bubbles, first using an electric discharge and then a pulsed laser. Unfortunately, despite all the care given to the experimental setup, spherical bubbles can hardly be created on earth. In fact, the hydrostatic pressure gradient in

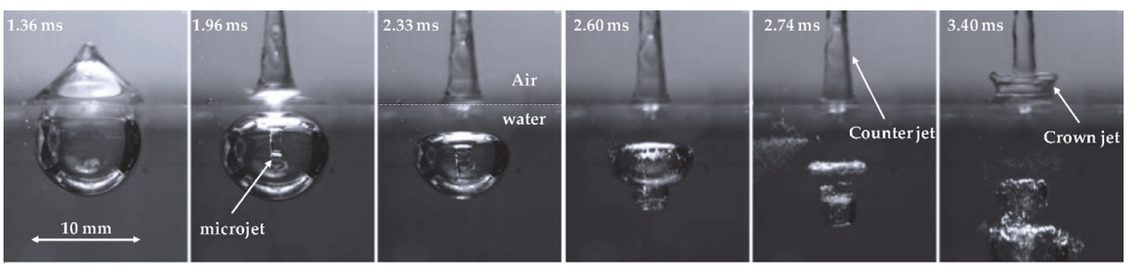

Figure 4.
Growth and collapse of a cavitation bubble near a free surface with the formation of jets inside the bubble and out of the surface.

the liquid caused by gravity will always deform the bubble. To cope with this limitation, one "simply" needs to get rid of gravity effects. This is precisely what parabolic flights can achieve. Running the tests in microgravity allows us to generate bubbles that are more spherical and explore the direct effect of different levels of gravity on their dynamics. So far, we took part in nine parabolic flight campaigns (PFC), eight organized by the ESA and one organized by a Swiss entity, as listed in **Table 1**.

Our experiment flies, with a dozen of other experiments, aboard an Airbus A310 (A300 before 2015), which was adapted to perform parabolic flight maneuvers. The microgravity campaign typically includes three flights, operated on three consecutive days. A typical flight lasts for about 2–4 h and includes 31 parabolas, each offering 20 seconds of microgravity. If requested, a series of steep turns may be also performed to generate stabilized hyper-gravity levels (e.g. 1.2, 1.4, 1.6 and 1.8 g). These maneuvers are illustrated in **Figure 5** with a typical evolution of the gravity level measured by an on-board accelerometer. It should be noted that the accumulated time spent in microgravity is only 10 min per flight! This highlights the importance of the thorough design and preparation of the setup, which should leave no room for failure. In particular, the experiment must be simple and automated as much as possible. During the parabolas, an operator can have difficulties controlling the experiment efficiently. Should operators become sick because of the awkward hyper-gravity phases, the experiment must be able to continue running without their intervention. In addition to the valuable assistance provided by parabolic flights experts, we also had the privilege to collaborate with Claude Nicollier (first Swiss astronaut) to improve these important but nonobvious aspects.

The flight day always starts at 6 a.m. with an ultimate check of the experimental setup using a well-honed procedure. The test chamber is filled with fresh water, and the test sequence is uploaded to the computer to allow for its automatic execution. 8 a.m. is the time for scopolamine injection. This medication is made available to flying participants to overcome the so-called space adaptation syndrome, also referred to as motion sickness. At 9 a.m. sharp, the doors are closed and the plane is ready to leave. About 30 min after take-off, the experimenters are allowed to leave

Year	2005	2006	2011	2012	2013	2014	2015	2015	2017
Campaign ID	SPFC 8	PFC 42	PFC 53	PFC 56	PFC 58	PFC 60	PFC 62	Swiss PFC 1	PFC 67

All flights departed from Bordeaux (France) except the Swiss PFC 1 (from Dübendorf, near Zurich, Switzerland).

Table 1.
List of attended parabolic flight campaigns.

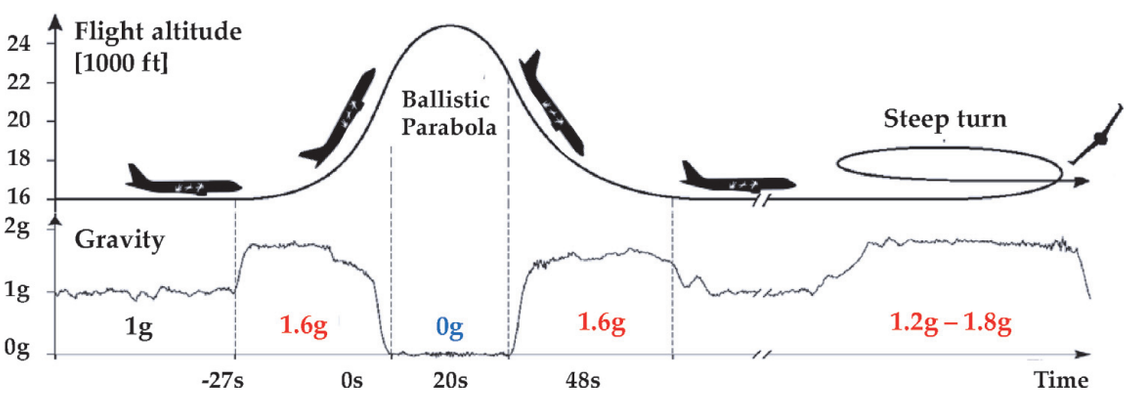

Figure 5.
Typical evolution of the vertical acceleration during parabola and steep turn maneuvers.

their seats to power up their experiments and get ready for the first parabola. This point of no return is probably the most stressful moment of the flight, definitely not suited for nervous fliers. Everyone tries to hide the palpable anxiety with all kinds of distractions until the captain announces in a lovely French accent "5, … , 3, 2, 1, pull up, … , 20, 30". The plane rears up to bring its altitude from 16,000 to 30,000 feet in only 20 s. During this unpleasant and long hyper-gravity phase (∼1.8 g), everybody remains perfectly still. Fortunately, we suddenly switch to something extraordinary. "… 40, injection". At 45° inclination, the pilots shut down the engines, and the plane is injected into a parabolic arc offering an extraordinary period of free fall with a wonderful and liberating sensation. Everyone in the plane is floating, laughing and even shouting as to replace the noise from the engine, which dropped suddenly. This is the most exciting moment of the flight, which lasts for only 20 brief seconds. Follows another hyper-gravity phase and the plane recovers its horizontal flight. The sequence restarts 2 min later with the same anxiety and happiness, except for those less fortunate who must remain seated at the back of the plane holding a sick bag. After landing, everybody gathers in a debriefing to report issues and prepare the next flight. We use the afternoon to collect data and fix various problems. Once back in our headquarters, we all discover the freshly collected data and debate it for hours. We always appreciated this moment of prolific exchange.

4. Bubbles in drops, from erosion to exploding stars!

4.1 Experimental setup

The first two parabolic campaigns (SPFC 8 and PFC 42) were dedicated to the investigations of cavitation bubble dynamics inside a water drop. Here, the use of microgravity flights is motivated by the possibility to generate a centimeter spherical drop of water, which is hard to achieve on earth. The experimental setup, presented in **Figure 6**, is made of a transparent test chamber, where the bubble and drop are generated, a high-speed camera (up to 120,000 frames per second) and a 100 Joule flashlight. At the start of the microgravity phase, detected by an accelerometer, water is gently expelled through a 1-cm-diameter pipe filled with foam to form a water drop of about 2 cm in diameter. At the end of this phase, which lasts for about 15 s, the drop remains attached to the injector tip. A cavitation bubble is

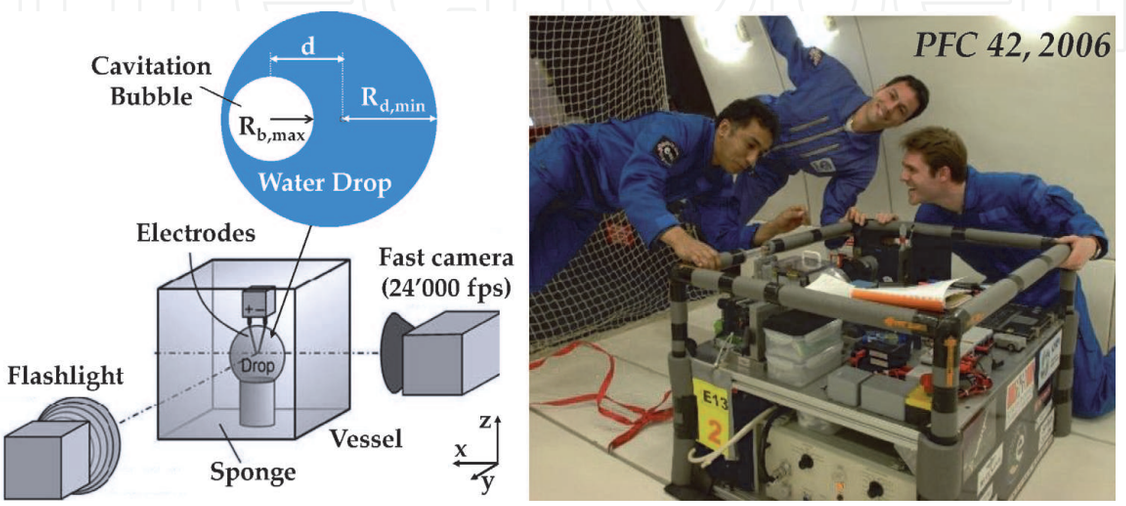

Figure 6.
Schematic of the bubble-in-drop experiment and a photo in microgravity.

then generated with the help of a spark electric discharge between two immersed platinum electrodes. The maximum radius of the bubble is varied by adjusting the discharge energy (up to 1 J). The governing parameters are the initial drop radius ($R_{d,min}$), the maximum bubble radius ($R_{b,max}$) and the eccentricity d.

4.2 Results

A sequence of high-speed visualization of a cavitation bubble within a $\sim$ 2 cm water drop is presented in **Figure 7**. We may observe how the electrical spark, visible on frame N°2, gives birth to an off-centred bubble, which expands to a maximum radius of $\sim$1 cm. The bubble then undergoes several collapses and rebounds, visible on frames N°13, N°21 and N°27. Interestingly, these frames reveal the formation of a myriad of short-lived microbubbles, which we do not observe for bubbles collapsing in a large volume of water. These transient microbubbles are due to confined shockwaves, which reflect on the drop surface and turn into tension waves. With the discovery of this *secondary cavitation*, we could propose a new path for the mechanism of erosion by a high-speed impact of water drops [7, 8], a recurring problem in various fields (e.g. rain erosion of wind turbines and aircrafts, steam turbines erosion, etc.). We argue that upon a high-speed impact of a water drop on a solid surface, the resulting shockwave travels inside the drop and turns into tension wave as it reflects on its boundary, leading to secondary cavitation, which is responsible of the erosion. To validate this hypothesis, we performed ground-based experiments with the precious help of the Swiss army. We visualized the impact of a 9 mm bullet on a $\sim$ 2 cm water jet. The result, illustrated in **Figure 8**,

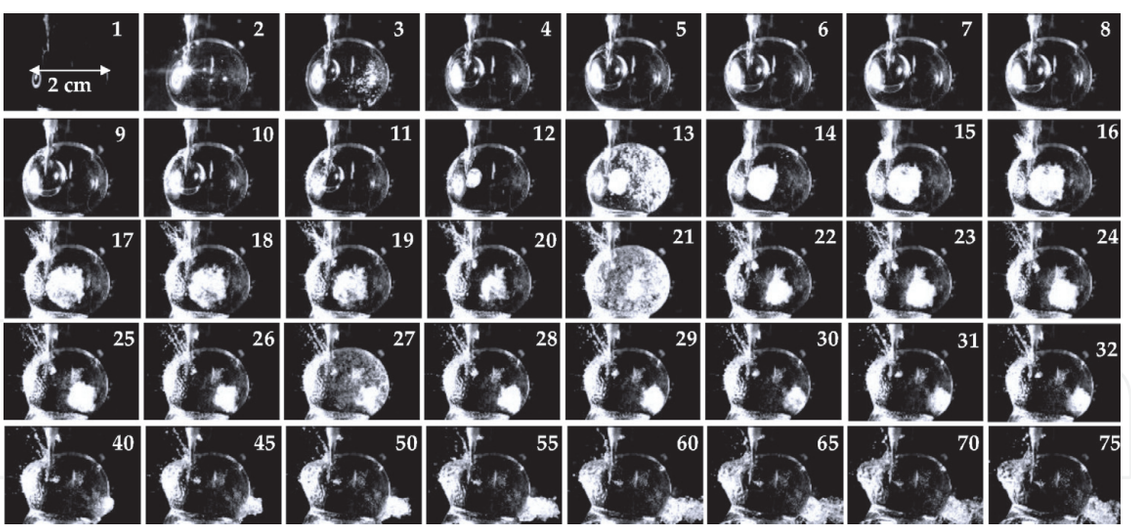

Figure 7.
Visualization of a bubble growth and collapse inside a water drop $R_{d,\min} = 2$ cm, $R_{b,\max} = 1$ cm. The inter-frame is 80 μs (400 μs for the last row).

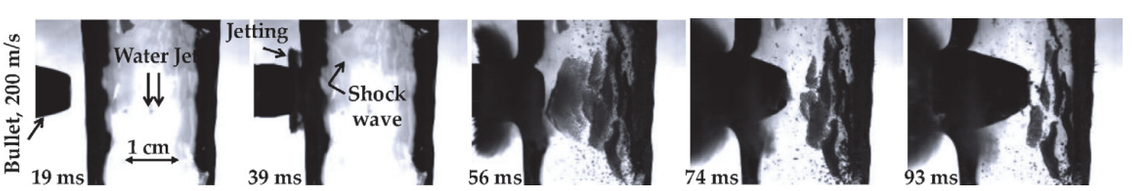

Figure 8.
Visualization of a high-speed impact of a 9 mm bullet on a $\sim$ 2 cm water jet. Evidence of secondary cavitation due to shockwaves confinement.

reveals the sudden formation of a large amount of cavitation bubbles within the jet, shortly after the bullet impact. The occurrence of this cavitation coincides perfectly with the passage of the reflected shockwave, visible on the third frame.

The sequence of **Figure 7** also reveals that as the bubble collapses and rebounds, two opposite jets emerge from the drop. The first one is the so-called counter-jet or splash. The second one results from the water entrained by the bubble as it moves away to the opposite side. Compared to the case of a bubble near a flat free surface (**Figure 4**), the counter-jet is wider and no crown jet is formed. This illustrates the role of the free surface curvature.

The evolution of the bubble radius, obtained by image processing, in the case a bubble in the centre of a 2 cm drop in microgravity, compared with a ground-based experiment in extended water volume is presented in **Figure 9**. We may observe that the collapse time is significantly shorter for the bubble-in-drop. We developed a theoretical model by extending the Rayleigh model and came up with an analytical solution that fits remarkably well with experimental data, as illustrated in the same figure. The details of this theory can be found in [9].

Another fascinating and peculiar outcome of the bubble-in-drop experiments in microgravity is the intriguing similarity found with the type II supernova Cas A, one of the most prominent stellar explosions in our Galaxy in human history [10]. Type II supernovae, also known as "core-collapse supernovae", occur when the iron core of a massive star (>8 solar masses) can no longer support its own weight and collapses within a matter of seconds at a quarter of the speed of light. This event triggers the collapse of the outer shells, causing a violent explosion of the star, temporarily boosting its luminosity a millionfold. Kinematic and chemical analyses of such "supernova remnants" allow us to decipher the physics of the explosion. In the case of Cas A, the pair of jets shown in **Figure 10** remains hard to explain. Despite the limited comparability of these jets to those observed in our water drops, the striking qualitative similarity nonetheless raises the question if Cas A might have been caused by an *eccentric* core collapse, for instance caused by a nearby companion star. Computer simulations are underway to investigate such scenarios.

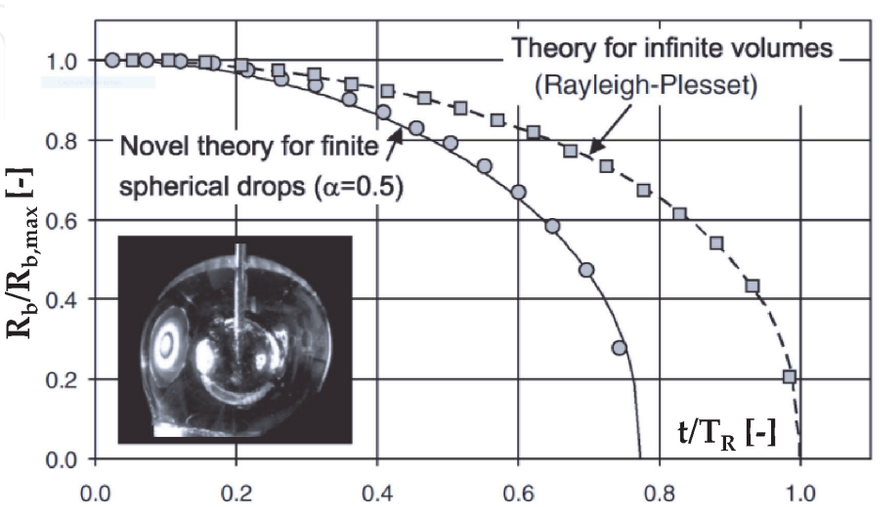

Figure 9.
Evolution of normalized radius of a bubble collapsing in the centre of a ~2 cm water drop. Symbols: experimental data. Dashed line: Rayleigh theory. Solid line: Novel theory for bubbles in drops [9].

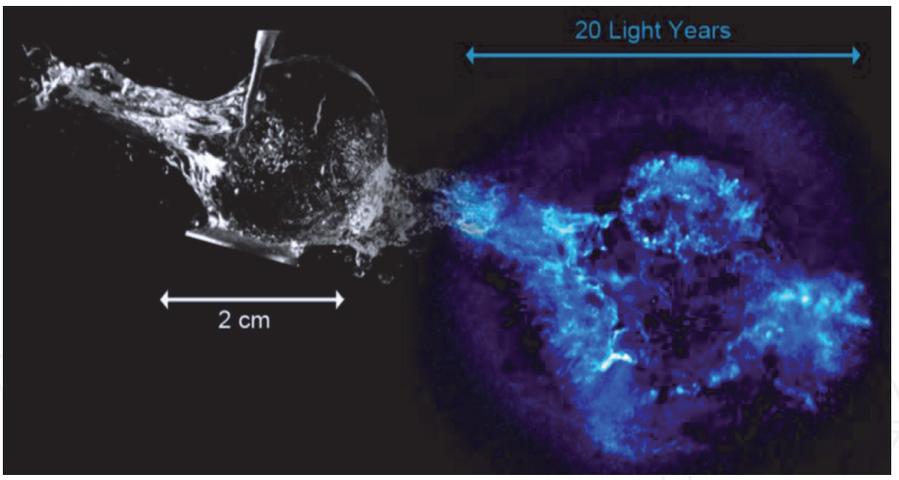

Figure 10.
Analogy of a bubble-in-drop with a massive star explosion (Cas A supernova remnant, viewed by Chandra X-ray Observatory *[10]).*

5. Gravity effects on cavitation bubble dynamics

5.1 Experimental setup: the quest for the most spherical bubble

We provide hereafter an overview of microgravity experiments, covering the periods 2011–2017, during which we took part in seven parabolic flight campaigns (see **Table 1**). We have designed a versatile experimental setup, which produces a single cavitation bubble in still water with a highly spherical shape. The setup is suited for both ground and microgravity flights and fulfills the ESA requirements, related to security and energy consumption as well as volume and payload limitations. We used two conventional racks to host our experiment. The total weight and volume are ~300 kg and ~0.6 m^3, respectively. A special attention was paid to reinforce the mechanical structure of the racks (i) to withstand a maximum acceleration of 9 g, as imposed by the ESA, and (ii) to avoid deformations due to gravity changes, which may alter the delicate optical alignment.

Bubble generation: Our setup generates one bubble at a time in the centre of an 18 × 18 × 18 cm acrylic chamber, filled with distilled water. The bubble is induced by focusing a pulsed laser of 532 nm wavelength, 8 ns duration and a 230 mJ maximum energy per pulse. As illustrated on **Figure 11**, the laser is first enlarged to a diameter of 51 mm using a beam expander. It is then focused with the help of a parabolic mirror immersed in water. The resulting pointlike plasma leads to the growth of a highly spherical bubble. The absolute pressure within the test chamber may be varied from atmospheric pressure down to 0.1 bar, with a vacuum pump.

Obviously, carrying a Class IV laser and 10 L of water in a confined microgravity aircraft does not go unnoticed, and we have to obey strict security rules. To this end, the main rack, which hosts the laser and the water chamber, is sealed to prevent water leakage and generously painted in black to minimize laser reflections. The rack is also equipped with interlocks to cut the electric power whenever the top lid is open.

The entire experiment is controlled by a laptop, which monitors the gravity level and starts the sequence as soon as the predefined level of gravity is reached. Although the duration of the microgravity phase (20 s) is long enough to repeat the test several times, we only do it once. In fact, in the absence of gravity, the residual gas after the bubble collapse remains in the centre of the chamber and does not rise upwards as it does on earth. It is then impossible to focus the laser in a mixture of

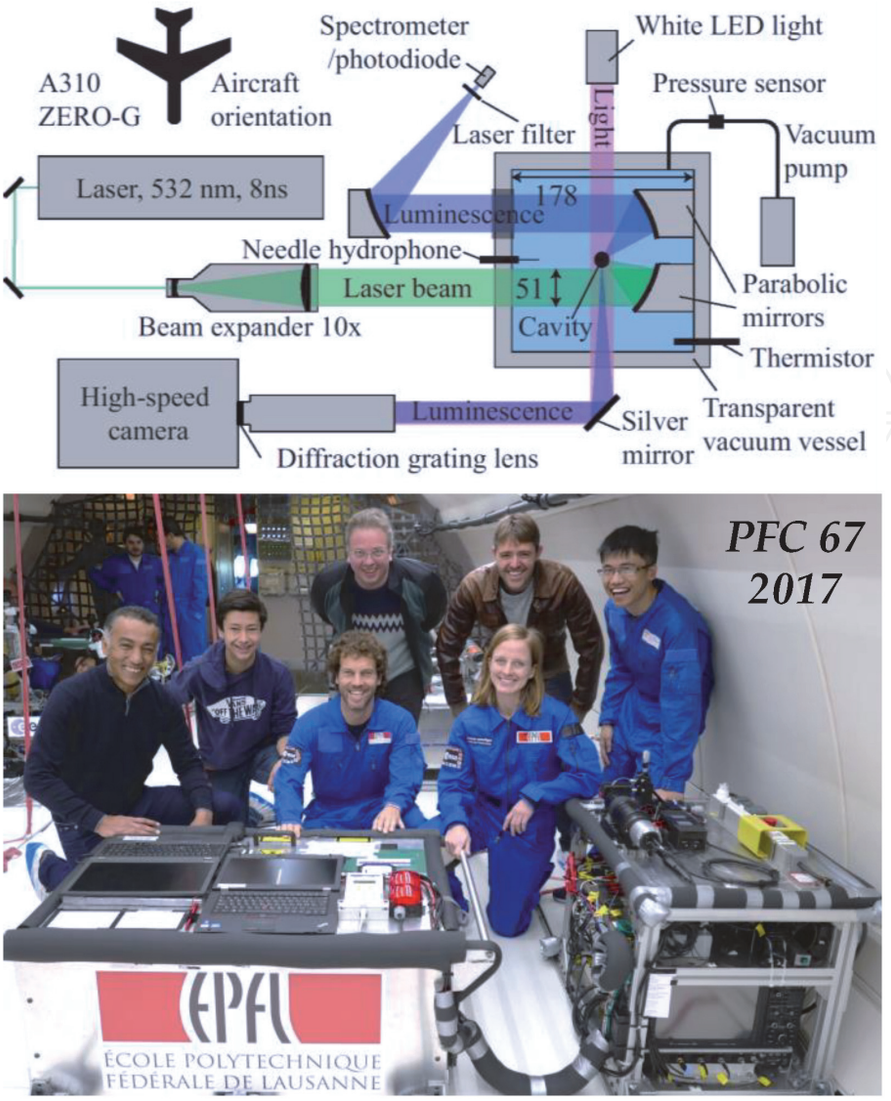

Figure 11.
(Top) schematic of the experimental setup (the dimensions are in mm) and (bottom) view of the two racks attached to the aircraft.

liquid and gas efficiently. Besides the microgravity phase, we also use hyper-gravity phases to widen the parameter space.

We implemented several sensors in the main rack to monitor various parameters during the experiment. A g-sensor is attached to the rack to measure the acceleration with a precision of ~0.2%. The resulting signal is used to start a predefined test sequence as soon as a prescribed level of gravity is reached. This sensor plays a major role in automating the experiment. A typical evolution of the gravity level during parabolic and hyper-gravity sequences is illustrated in **Figure 5**. The water temperature is measured with a thermometer, immersed in the chamber. The temperature is a key parameter for the dynamics of cavitation bubbles since it governs the pressure thresholds and rates of vaporization and condensation as well as the concentration of dissolved gas.

High-speed visualization: The follow-up of the bubble expansion, collapse and rebound as well as the visualization of radiated shockwaves is performed with a high-speed camera, fitted in the main rack as shown in **Figure 11**. A 7 W LED source, opposite to the camera, provides a slightly diverging light beam. Such a configuration requires much less light and makes it possible to view the shockwave passage, because the density gradient at their front deviates the light (shadowgraph). The imaging system can reach up to 10 million frames per second and the

minimum exposure time is 50 ns. The image resolution is 400 × 250 pixels for all frame rates. The high-speed performance of Shimadzu camera is due to its complementary metal-oxide-semiconductor (CMOS) burst image sensor, which hosts the pixels and the memory in the same chip. While this technology reduces the transfer time, it offers a limited number of frames (250). Therefore, we have developed a methodology to provide a precise triggering of the camera and explore various phases of its lifetime. To this end, we have used shockwave sensors, light detectors and a GHz oscilloscope to generate accurate trigger signals for the laser pulse ignition and the high-speed camera as well.

Shockwave sensors: The shockwaves generated at bubble initiation and collapse are measured by two highly sensitive piezoelectric needle hydrophones, placed at 34.3 mm and 35.7 mm away from the bubble centre. The measurement bandwidth is ~20 MHz, which makes it possible to follow the rapid change of the pressure during the shock passage. The hydrophones offer a very precise signal to post-trigger the high-speed camera.

Luminescence detection: Another spectacular aspect of cavitation bubble dynamics that we have investigated in microgravity is the luminescence released at the final stage of the collapse. We have tracked luminescence in both time and frequency domains. A major innovation lies in the use of two parabolic mirrors, located inside and outside the water chamber, which improves significantly the signal-to-noise ratio. At the focal point of the second mirror, we have placed a notch filter and an optic fiber, which leads the light to a spectrometer. To allow for time-resolved measurements, the spectrometer is replaced by a fast silicon photodetector, having 1 ns rise time and a range of 200–1100 nm wavelength.

5.2 Major results

We provide here a selection of the most important results obtained with the experimental setup explained above. Interested readers may refer to the more in-depth publications by the *Flash and Splash* team [11–25].

5.2.1 Effects of pressure anisotropy on collapse-induced jets

Thanks to microgravity experiments, we could provide for the first time the evidence of gravity effects on cavitation bubble dynamics. **Figure 12** illustrates the growth and collapse of three bubbles generated with the same laser energy and surrounding pressure at three gravity levels (1 g, 1.6 g and 0 g). We may clearly observe that the bubble in microgravity remains spherical through the collapse and rebound phases while the two other bubbles develop an upward jet during the rebound phase. The latter is more pronounced in hyper-gravity. We may also observe that as the gravity level is increased, the maximum bubble radius decreases, and the centroid of the rebound bubble moves upwards (buoyancy).

The upward jet is due to the difference of hydrostatic pressure between the upper and lower parts of the bubble. The liquid beneath the bubble moves naturally faster towards the bubble centre, leading to interface instability and jet formation. While such explanation holds for large bubbles, it is not clear how far the gravity-induced pressure gradient can influence smaller bubbles. We carried out a large number of experiments involving bubbles of different sizes, subjected to different driving pressures and gravity levels. We have also performed ground-based experiments in the presence of free and solid surfaces. Here again, the bubble size and driving pressure were varied in a wide range. Moreover, we carried out potential flow simulations, using the boundary integral method (BIM). The analysis of a large number of experimental and numerical data, combined with theoretical

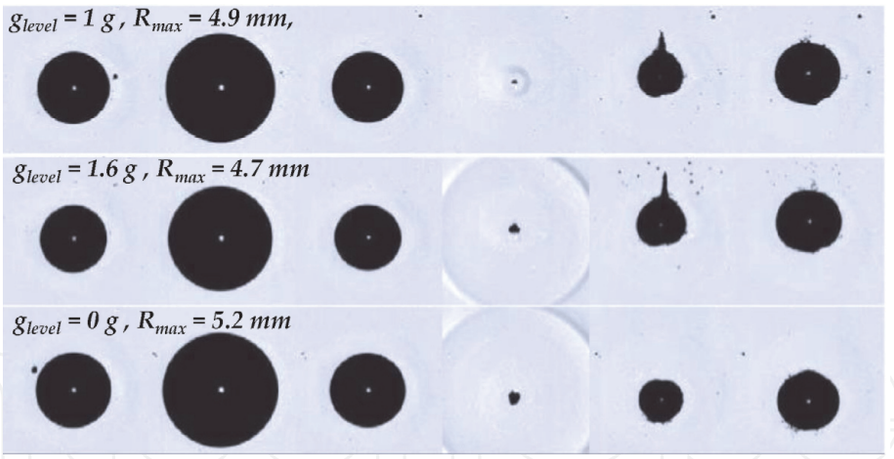

Figure 12.
Three bubbles generated in water with the same laser energy and driving pressure (10 kPa), but at three different gravity levels (adapted from [2]).

considerations, led us to propose a unified framework to predict the bubble deformation and jet properties. Our approach is based on an anisotropy parameter ζ, which is a non-dimensional representation of the so-called Kelvin impulse, i.e. the linear momentum acquired by the liquid during the asymmetric growth and collapse of the bubble. We managed to express this parameter (ζ) in its vector form, for all tested configurations as follows:

$$\boldsymbol{\zeta} = \begin{cases} -\rho \boldsymbol{g} R_0 \Delta p^{-1} & \text{gravitational field} \\ -0.195\gamma^{-2}\boldsymbol{n} & \text{flat rigid surface} \\ +0.195\gamma^{-2}\boldsymbol{n} & \text{flat free surface} \end{cases}$$

where ρ is the liquid density, $\boldsymbol{g}$ is the gravity vector, R_0 is the maximum bubble radius, and $\boldsymbol{n}$ is the unit vector normal to the neighboring surface and directed towards the bubble centre. The so-called stand-off parameter (γ) is defined as h/R_0, where h is the distance between the bubble centre and the boundary.

We have identified three different regimes for the jet induced by a collapsing bubble: weak, intermediate and strong. Weak jets occur for slightly deformed bubbles $\left(\zeta < 10^{-3}\right)$ and are hardly visible throughout the collapse and rebound. Intermediate jets $\left(10^{-3} < \zeta < 0.1\right)$ pierce the opposite bubble wall at the end of the collapse phase and emerge during the rebound. Such jets occur for large bubbles subjected to gravity as illustrated on **Figure 12**. Strong jets $(\zeta > 0.1)$ develop earlier and pierce the bubble way before the end of the collapse phase (see illustrations in the case of a bubble near a free surface in **Figure 4**).

The dynamics of the jet is systematically analyzed through different properties, such as the jet impact time, jet speed, bubble displacement, bubble volume at jet impact and vapor-jet volume. We found that, once properly normalized, these variables reduce to straightforward functions of ζ, in fair agreement with numerical simulations. An illustration is given in **Figure 13** for the normalized jet velocity.

Interestingly, we obtain simple approximations of the jet properties as functions of the parameter ζ, regardless of jet drivers (gravity/neighboring boundaries) and over a wide range of ζ. Here are the approximations found for the jet velocity, the bubble displacement and the jet impact time:

- Normalized jet speed: $U_{jet}/\sqrt{\Delta p/\rho} \approx 0.9\zeta^{-1}$

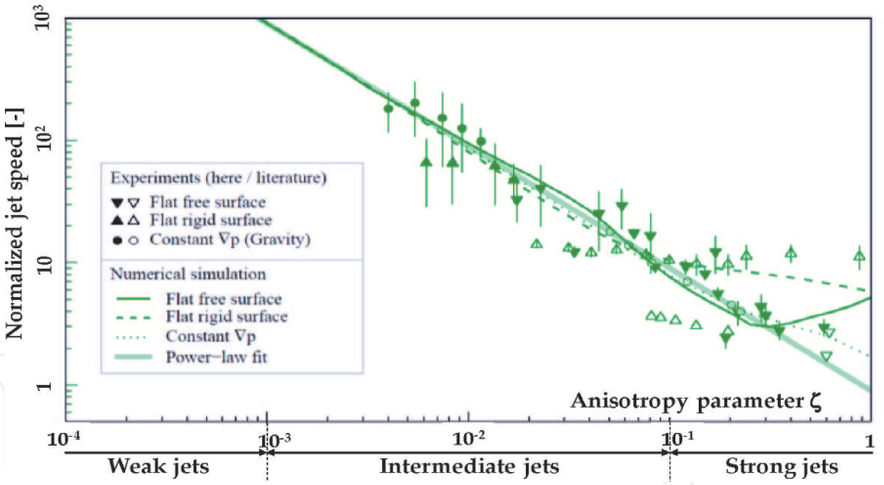

Figure 13.
Normalized jet speed ($U_{jet}/\sqrt{\Delta p/\rho}$) as a function of ζ and γ. Our data (filled symbols) are compared with literature data (empty symbols). The lines are the numerical models. The thick line is the power-law fit (adapted from [3]).

- Normalized bubble displacement: $\Delta z/R_0 = 2.5\zeta^{3/5}$
- Jet impact time scaled by collapse time: $T_{\mathrm{Impact}}/T_{Collapse} \approx 0.15\zeta^{5/3}$

5.2.2 Effects of pressure anisotropy on shockwaves

We have found that the formation of shockwaves is also highly sensitive to the bubble deformation induced by pressure anisotropy. In microgravity, the bubble remains spherical throughout the collapse phase with an emission of a single and intense shockwave, as illustrated in **Figure 14**. We have plotted on the same figure the case of a bubble deformed by a neighboring free surface ($\zeta = 0.19$). For such high

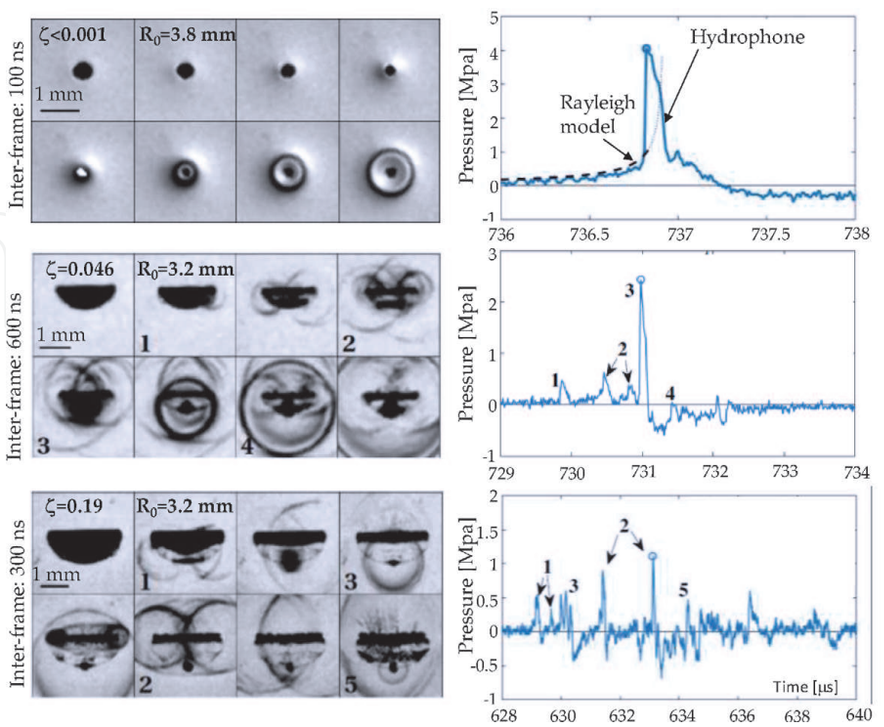

Figure 14.
Visualization of three collapsing bubbles and the corresponding pressure signal recorded by the hydrophone. The shockwaves are denoted by 1, jet impact; 2, torus collapse; 3, tip bubble collapse; 4, second torus collapse; and 5, second tip bubble collapse (adapted from [3]).

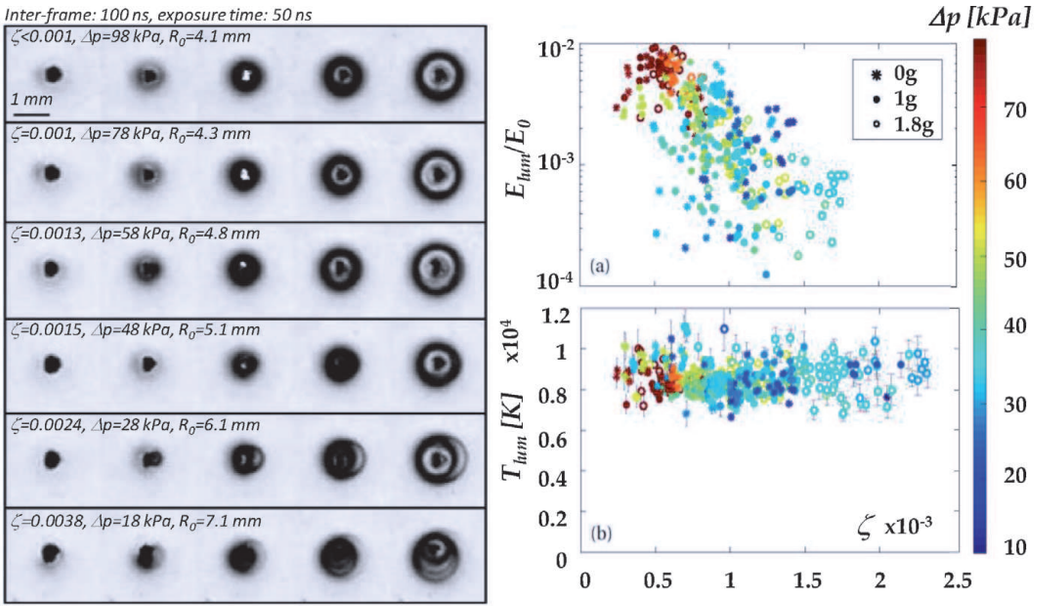

Figure 15.
Left: visualization of luminescence emitted by a collapsing bubble, for different values of ζ. Right: single bubble luminescence (a) relative energy E_{lum}/E_o *and (b) blackbody temperature* T_{lum} *vs. ζ. Colors indicate the driving pressures, and symbols indicate the different levels of gravity (adapted from [3]).*

anisotropy parameter, a strong jet develops and fractions the cavity into a tip cavity and a toroidal cavity. We observe the emission of several shockwaves related to jet impact and the collapse of the bubble fragments. These events are identified in the corresponding pressure signal. We found that the energy radiated by the shockwaves is maximum for the spherical collapse case and decreases with deformed bubbles.

5.2.3 Effects of pressure anisotropy on luminescence

The direct visualization of luminescence emitted by the collapse of a cavitation bubble in normal gravity is presented in **Figure 15** for different values of the anisotropy parameter ζ. The latter was varied by adjusting the driving pressure. We may observe that luminescence is generated when the bubble reaches its minimum radius, just before the shockwave emission. The figure clearly illustrates how luminescence fades away as the bubble is deformed.

We have processed a large number of broadband spectra of luminescence emitted by individual laser-induced bubbles, collapsing in different gravity-induced pressure gradients. As shown in **Figure 15**, we found that the luminescence energy E_{lum}, normalized by the potential energy of the bubble E_0, varies in a roughly exponential way with ζ. We assumed the blackbody radiation to estimate the temperature reached by the noncondensable gas within the bubble. Our results, presented in the same figure, confirm the high values of gas temperature, which ranged between 7000 and 11,500 K. We may also observe that the luminescence ceases for a threshold value, which coincides with the transition from weak to intermediate jets. Nevertheless, unlike the luminescence energy, we have found no clear variation of the blackbody temperature as a function of ζ. This counter-intuitive result needs further investigations to be clarified.

6. Conclusion

During their brief and violent life, cavitation bubbles may develop powerful phenomena and cause damage in a variety of industrial devices. Nevertheless, by

mastering their unique ability to focus energy, cavitation bubbles may be beneficial in many applications, such as cleaning, chemistry, material and food processing and medicine. The present chapter provides a summary of our research activities related to this fascinating topic and underlines the valuable contribution of microgravity experiments. This review covers the past 15 years, during which we have participated in nine parabolic flight campaigns.

We first investigated the case of a bubble-in-drop and discovered how an eccentric collapse leads to the formation of two opposite liquid jets, which amazingly resemble the ones observed during the collapse of giant stars. We also learned how the shockwave confinement generates secondary cavitation, which provides a better understanding of the erosion due to a high-speed impact of liquid drops (rain erosion). Moreover, we developed and validated a new theory for bubble dynamics within a liquid drop.

To explore the final stage of a bubble collapse, we built a versatile experimental setup, which generates a single cavitation bubble by focusing a pulsed laser in a water chamber. The combination of a careful design of the optical setup and the use of microgravity flights let us produce the most spherical bubbles, hardly achievable in ground-based experiments. We also used variable gravity offered by parabolic flights to modulate the hydrostatic pressure gradient and explore its effects on bubble deformation in a broad parameter space. We developed a unified theoretical framework to predict the dynamics of a cavitation bubble, based on a non-dimensional anisotropy parameter (ζ). We have found that the collapse of a spherical bubble ($\zeta \approx 0$) generates a unique and strong shockwave, no jetting and a rather small rebound. As ζ is increased, the bubble becomes more and more deformed with a more complex set of shockwaves, a larger rebound and a microjet that develops earlier and earlier. We also observed a rapid quenching of the collapse-induced luminescence for increasing ζ. Our model predicts how the energy in the initial cavitation bubble is partitioned between the collapse channels, namely, the shockwave, the jet, the rebound and the luminescence. This paves the way to optimize the outcome of a collapsing bubble, depending on the application.

The present chapter was written during the "great lockdown". Outside, the coronavirus disease 2019 (COVID-19) pandemic is raging around the world with dramatic consequences. Who knows? Maybe the solution will come from cavitation bubbles. If carefully injected into the human body and appropriately controlled by an acoustic field, microbubbles can locally deploy their extraordinary power to target and neutralize coronavirus with minimal side effects. Given the state of knowledge on cavitation bubbles, this is not wishful thinking.

Acknowledgements

On behalf of *Flash and Splash* team, I would like to express my gratitude to the European Space Agency for giving us the wonderful opportunity to fly our experiment in microgravity. I am also thankful to the parabolic flight experts for their assistance during the flight campaigns. The project received financial support from the Swiss National Science Foundation (grants no. 116641 and 513234), the European Union (H2020, grant no. 813766), the EPFL Space Centre, the University of Western Australia and Breitling AG.

Notes/thanks/other declarations

The *Flash and Splash* project would not have been possible without the perseverance and commitment of D. Obreschkow, Ph. Kobel, N. Dorsaz and A. De

Bosset, the outstanding contributions of M. Tinguely and O. Supponen and the precious assistance of EPFL technicians (L. Bezençon, M. Raton and R. Fazan). I would like to thank them all warmly.

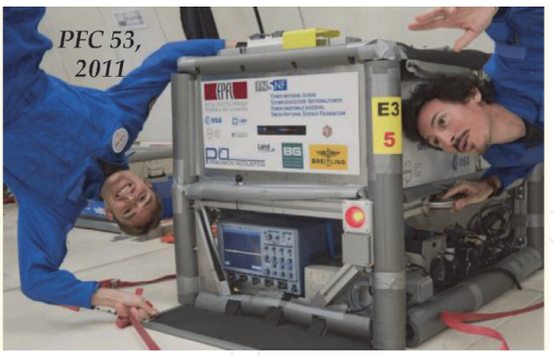

Author details

Mohamed Farhat
Ecole Polytechnique Fédérale de Lausanne, Switzerland

*Address all correspondence to: mohamed.farhat@epfl.ch

References

[1] Robert E, Lettry J, Farhat M, Monkewitz PA, Avellan F. Cavitation bubble behavior inside a liquid jet. Physics of Fluids. 2007;**19**(6):067106

[2] Tinguely M. The effect of pressure gradient on the collapse of cavitation bubbles in normal and reduced gravity. [EPFL PhD thesis N°5674]; Switzerland: Ecole Polytechnique Fédérale de Lausanne; 2013

[3] Supponen O. Collapse phenomena of deformed cavitation bubbles. [PhD Thesis N°8089]; Switzerland: Ecole Polytechnique Fédérale de Lausanne; 2017

[4] Franc P et al. La Cavitation: Mécanismes Physiques et aspects Industriels. France: EDP Sciences; 1995. ISBN: 978-2-86883-451-5

[5] Koukouvinis PH, Bruecker CH, Gavaise M. Unveiling the physical mechanism behind pistol shrimp cavitation. Scientific Reports. 2017;**7**: 13994. DOI: 10.1038/s41598-017-14312-0

[6] Rayleigh L. On the pressure developed in a liquid during the collapse of a spherical cavity. Philosophical Magazine. 1917;**34**(200):94-98

[7] Field JE, Camus J-J, Tinguely M, Obreschkow D, Farhat M. Cavitation in impacted drops and jets and the effect on erosion damage thresholds. Wear. 2012;**290–291**:154-160

[8] Obreschkow D, Dorsaz N, Kobel P, De Bosset A, Tinguely M, Field J, et al. Confined shocks inside isolated liquid volumes: A new path of erosion? Physics of Fluids. 2011;**23**:101702

[9] Obreschkow D, Kobel P, Dorsaz N, De Bosset A, Nicollier C, Farhat M. Cavitation bubble dynamics inside liquid drops in microgravity. Physical Review Letters. 2006;**97**: 094502

[10] Hwang U et al. A million second Chandra view of Cassiopeia A. The Astrophysical Journal. 2004;**615**: L117-L120

[11] Supponen O, Obreschkow D, Kobel P, Dorsaz N, Farhat M. Detailed experiments on weakly deformed cavitation bubbles. Experiments in Fluids. 2019;**60**:33

[12] Supponen O, Akimura T, Minami T, Nakajima T, Uehara S, Ohtani K, et al. Jetting from cavitation bubbles due to multiple shockwaves. Applied Physics Letters. 2018;**113**:193703

[13] Supponen O, Obreschkow D, Farhat M. Rebounds of deformed cavitation bubbles. Physical Review Fluids. 2018;**3**:103604

[14] Supponen O, Obreschkow D, Kobel P, Farhat M. Luminescence from cavitation bubbles deformed in uniform pressure gradients. Physical Review E. 2017;**96**(3):033114

[15] Supponen O, Obreschkow D, Kobel P, Tinguely M, Dorsaz N, Farhat M. Shock waves from nonspherical cavitation bubbles. Physical Review Fluids. 2017;**2**(9):093601

[16] Supponen O, Obreschkow D, Tinguely M, Kobel P, Dorsaz N, Farhat M. Scaling laws for jets of single cavitation bubbles. Journal of Fluid Mechanics. 2016;**802**:263-293

[17] Koukouvinis P, Gavaises M, Supponen O, Farhat M. Simulation of bubble expansion and collapse in the vicinity of a free surface. Physics of Fluids. 2016;**28**(5):052103

[18] Koukouvinis P, Gavaises M, Supponen O, Farhat M. Numerical

simulation of a collapsing bubble subject to gravity. Physics of Fluids. 2016;**28**(3): 032110

[19] Supponen O, Kobel P, Obreschkow D, Farhat M. The inner world of a collapsing bubble. Physics of Fluids. 2015;**27**(9):091101

[20] Obreschkow D, Tinguely M, Dorsaz N, Kobel P, De Bosset A, Farhat M. The quest for the most spherical bubble: Experimental setup and data overview. Experiments in Fluids. 2013;**54**(4):1503

[21] Sato T, Tinguely M, Oizumi M, Farhat M. Evidence for hydrogen generation in laser- or spark-induced cavitation bubbles. Applied Physics Letters. 2013;**102**(7):074105

[22] Tinguely M, Obreschkow D, Kobel P, Dorsaz N, De Bosset A, Farhat M. Energy partition at the collapse of spherical cavitation bubbles. Physical Review E. 2012;**86**(4):046315

[23] Obreschkow D, Bruderer M, Farhat M. Analytical approximations for the collapse of an empty spherical bubble. Physical Review E. 2012;**85**(6): 066303

[24] Obreschkow D, Tinguely M, Dorsaz N, Kobel P, De Bosset A, Farhat M. Universal scaling law for jets of collapsing bubbles. Physical Review Letters. 2012;**107**(20):204501

[25] Kobel P, Obreschkow D, De Bosset A, Dorsaz N, Farhat M. Techniques for generating centimetric drops in microgravity and application to cavitation studies. Experiments in Fluids. 2009;**47**(1):39-48